

## [Review Paper]

# Measurement of Vacuum Residue and Asphaltene Fluid Properties at Process Conditions

Murray R. GRAY\*, Janet A. W. ELLIOTT, and William C. McCAFFREY

Dept. of Chemical and Materials Engineering, University of Alberta, Edmonton, AB T6G 2G6, CANADA

(Received November 1, 2004)

The fluid properties of interfacial tension and viscosity, and the fluid-solid interactions embodied in the contact angle, are important in a wide range of phenomena that affect the processing of the vacuum residue fractions of petroleum and oilsand bitumens. Direct measurements of these fluid properties at representative processing conditions can give important insight into a variety of design and operating challenges, from gas holdup in hydroconversion to fouling of furnace tubes. This review summarizes the efforts to measure fluid properties of vacuum residue materials at high temperature and pressure. Significant progress has been made in measuring surface tension and viscosity of vacuum residues at temperatures to 530°C at low pressures. Further work is needed to develop methods for measurement of contact angle, and for measurements at high pressure.

**Keywords**

Fluid property, Surface tension, Viscosity, Contact angle, Vacuum residue, Asphaltene

**1. Introduction**

The vacuum residue fraction of petroleum, comprising material with a normal boiling point of over 524°C, is a complex mixture of components with a wide range of molecular weight and chemical structure. The emphasis in process development and design for conversion of the vacuum residue fraction has tended to focus on the chemistry of the feed and the cracked products, and to some extent the chemistry of the transformation between the two. Most observations of the changes during the reactions of vacuum residue are based on laboratory measurements at room temperature and pressure. Consequently, we focus on the yields of solubility fractions such as the toluene-insoluble fraction (*i.e.* coke) and the toluene-soluble-heptane insoluble fraction (*i.e.* asphaltene), or the mesophase characteristics of the coke solids. To a significant degree, however, these observations fail to define some of the key fluid properties that govern the operation of reactor systems. In addition to defining the fluid phases that are present in a reactor during conversion of vacuum residue, we need to consider their interactions with each other, surfaces in the reactor, and catalysts. The properties of the vacuum residue fluids and reaction products that control these interactions are the viscosity, the surface tension and the contact angle.

This review will first summarize the phenomena in conversion of vacuum residue that depend critically on fluid properties, then present recent work on the measurement of fluid properties at actual reactor conditions. We will then close with a summary of the key fluid properties that remain to be determined.

**2. Fluid Properties in Residue Processing**

Refining of heavy petroleum fraction begins with distillation at temperatures over a range from 200°C up to approximately 350°C, and pressures of 5–150 kPa, followed by conversion at higher temperatures and pressures. Broadly speaking, therefore, the process conditions of interest for the behavior of residue span a temperature range from 200°C to over 500°C, and from vacuum conditions to 20 MPa hydrogen pressure or even higher. Each technology for conversion of vacuum residue has its own particular operating challenges, but they are all linked by some common phenomena at the level of fluid properties. **Table 1** lists the main technologies for conversion of vacuum residue, and the aspects of design and operation that are most influenced by fluid properties in each case.

Many of these fluid-related phenomena also involve chemical reaction, so that the phases that are present in the reactor, and their fluid properties, are strongly dependent on the reactions of the feed material. For example, fouling of furnace tubes in delayed coking involves a complex combination of fluid phase and sur-

\* To whom correspondence should be addressed.

\* E-mail: murray.gray@ualberta.ca

Table 1 Fluid Property-related Phenomena in Residue Conversion

Conversion process	Fluid property-related phenomena
Delayed coking (450-500°C, 100-300 kPa)	Furnace and transfer line fouling (combination of reaction and deposition from fluid phase) Foaming in coke drum
Visbreaking (450-500°C, 100-300 kPa)	Furnace fouling Fouling of soaker coils or drums
Fluid coking (500-540°C, 100-200 kPa)	Atomization of liquid Agglomeration of coke particles by liquid feed Fouling of reactor internals Mass transfer in reacting liquid phase
Ebullated bed hydroconversion and slurry-phase hydroconversion (400-450°C, 10-20 MPa)	Gas holdup in reactor Gas bubble size and coalescence Wetting of catalyst by liquid phases (residue and coke)
Fixed-bed hydroconversion (400-430°C, 10-20 MPa)	Liquid holdup in the reactor Deposition of fine solids
Residue fluid catalytic cracking (470-520°C, 100-200 kPa)	Atomization of liquid Liquid contact with catalyst and wetting

Table 2 Fluid-mechanic Interactions in Vacuum Residue Conversion

Interaction	Dimensionless groups	Fluid properties
Liquid droplet formation	Weber number, $We = \frac{\rho U^2 d}{\sigma}$ Reynolds number, $Re = \frac{dU\rho}{\mu}$ Ohnesorge number, $Oh = \frac{\sqrt{We}}{Re}$	Viscosity, surface tension
Bubble formation and coalescence	Eotvos number or Bond number, $Eo = \frac{g(\rho_L - \rho_G)d^2}{\sigma}$ Reynolds number, $Re = \frac{dU\rho}{\mu}$	Surface tension, viscosity
Liquid wetting of fine or porous solids (coke or FCC catalyst)	Capillary number, $Ca = U\mu/\sigma$ Contact angle, $\theta$	Viscosity, surface tension
Liquid wetting of surfaces (catalyst, reactor internals)	Weber number, $We = \frac{\rho U^2 d}{\sigma}$ Reynolds number, $Re = \frac{dU\rho}{\mu}$ Contact angle, $\theta$	Surface tension or interfacial tension, viscosity

face reactions, heat transfer, and transport of components to the furnace wall<sup>1)</sup>. The list of phenomena in **Table 1** can be further classified based on the underlying fluid-mechanical interactions. These interactions are dominated by interfacial phenomena, which control the dispersion of phases as bubbles and drops, coalescence, and wetting of solids by the fluid phases. The list in **Table 2** lists these underlying processes, and the controlling dimensionless groups and fluid properties.

Asphalts, vacuum residue, bitumens and crude oils are predominantly Newtonian fluids over a wide range of flow conditions, therefore, the viscosity is the most

important flow-related characteristic of these materials regardless of the time scale of the process. Surface and interfacial tension, on the other hand, can exhibit significant time dependence depending on the rate of change of interfacial composition. The classic example is the dynamic change in oil-water interfacial tension as a surfactant component partitions at the interface. In rapid processes, such as atomization of liquids in a jet, the dynamic surface tension of a multi-component mixture is more important than the equilibrium surface tension. An important dimensionless group for droplet behavior is the Ohnesorge number,

which is the ratio of viscous to interfacial forces on a fluid.

One important property of fluids is uniquely different from the rest in **Table 2**, and that is the contact angle between two fluids on a solid surface. The equilibrium, advancing, and receding contact angles are important in the wetting phenomena that can lead to fouling of reactor surfaces and catalysts. The Young equation defines the contact angle for two fluids at a solid surface at equilibrium:

$$\cos\theta = \frac{\sigma_{L1-S} - \sigma_{L2-S}}{\sigma_{L1-L2}} \quad (1)$$

where  $\sigma_{L1-L2}$  is the interfacial tension between the two fluid phases. A fundamental problem in systematically applying this relationship is that the surface energies of the solid-fluid interactions, and hence the solid-fluid interfacial tensions, are much more difficult to predict than fluid-fluid interfacial tension.

Given the importance of fundamental fluid properties in a range of conversion technologies, the following sections will review the efforts to measure surface tension, viscosity, and contact angle of vacuum residue at processing conditions.

### 3. Surface Tension

Several techniques have been used to measure surface and interfacial tensions of heavy oils and bitumens up to 200°C, including the spinning drop method, sessile drop and pendant drop techniques. The main requirement for these methods is that the surrounding fluid must be transparent.

Li *et al.*<sup>2)</sup> successfully extended the pendant drop method to measure the dynamic and equilibrium surface tensions of Athabasca vacuum residue (500°C+) up to 280°C at atmospheric pressure. They used the axisymmetric drop shape analysis (ADSA) pendant drop technique<sup>3,4)</sup> which uses an image of a pendant drop and fits the Laplace equation of capillarity to the measured drop profile. Li *et al.*<sup>2)</sup> measured dynamic surface tension of vacuum residue in the presence of nitrogen at 150 to 280°C. They also defined the role of atmospheric and dissolved oxygen as a confounding factor in measurements at these temperatures, presumably due to chemical oxidation. They observed a significant, slow, change from the initial values of surface tension to the equilibrium values, as shown in **Fig. 1**. The change of equilibrium surface tension of nitrogen-saturated Athabasca vacuum residue (AVR) with temperature is presented in **Fig. 2**. A linear relationship between surface tension and temperature was observed in the temperature range of 150 to 280°C. The decrease in equilibrium surface tension with increasing temperature is given by Eq. (2):

$$\sigma_{eq} \text{ (mN/m)} = 24.45 - 0.0248T \text{ (}^\circ\text{C)} \quad (2)$$

This equation follows the expected trend of linear

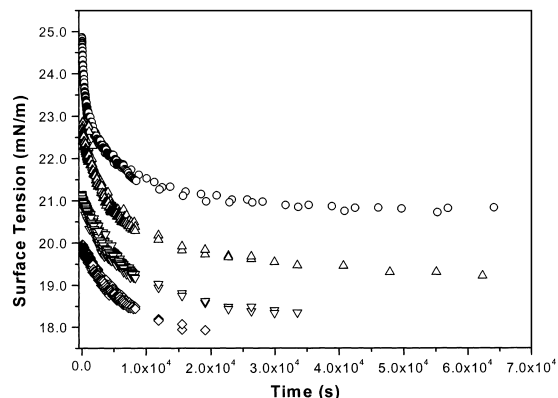


Fig. 1 Measured Dynamic Surface Tensions for Nitrogen-saturated Athabasca Bitumen Vacuum Residue (500°C+) in Contact with Nitrogen at 1 atm (○ 150°C; △ 200°C; ▽ 250°C; ◇ 280°C), from Li *et al.*<sup>2)</sup>

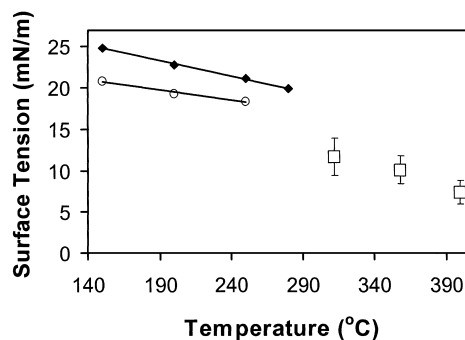


Fig. 2 Surface Tension of Athabasca Vacuum Residue (at 46 s) (◆) and Equilibrium (○) Surface Tensions by Pendant Drop Method for 150-280°C, and from the Liquid-bridge Method for Solids-free Athabasca Vacuum Residue (□) at 310-400°C (pendant drop data from Li *et al.*<sup>2)</sup> and liquid bridge data from Asprino<sup>11)</sup>)

decrease in surface tension with temperature<sup>5)</sup>.

The data of **Fig. 2** emphasize the importance of time-scale in selection of appropriate surface tension data. For rapid processes, such as fluid atomization in a nozzle, the initial surface tension would be most reasonable for modeling. An equilibrium value that is reached after several hours might be more relevant to slow fouling phenomena. The decreases from the initial surface tension values to equilibrium values are listed in **Table 3**, along with the time to the first measurement. The temperature dependence of the initial surface tension, measured after 46 s, is given by Eq. (3):

$$\sigma_{46sec.} \text{ (mN/m)} = 30.44 - 0.0376T \text{ (}^\circ\text{C)} \quad (3)$$

An obvious question from the data of **Fig. 1** is the cause for the slow time-dependent decrease in the surface tension. One reason would be an artifact due to viscous flow of the drop, but the viscosity of 45 to 320 mPa·s over this range of temperatures would not give such long transients. Consequently, the change illus-

Table 3 Effect of Temperature on Surface Tension of N<sub>2</sub>-saturated Athabasca Vacuum Residue in Contact with N<sub>2</sub>

Temperature [°C]	Surface tension [mN/m]		Decrease [%]	Initial rate [mN/m·s]
	Initial	Equilibrium		
150	24.86 ± 0.06	20.82 ± 0.04	16	8.4 × 10 <sup>-4</sup>
200	22.82 ± 0.08	19.31 ± 0.06	15	2.7 × 10 <sup>-4</sup>
250	21.10 ± 0.08	18.34 ± 0.06	13	1.4 × 10 <sup>-4</sup>
280	19.92 ± 0.07	17.8 <sup>a)</sup> , 17.5 <sup>b)</sup>	11	1.4 × 10 <sup>-4</sup>

Errors given are accuracy reported by the ADSA software.

a) Last value measured.

b) Estimated from Eq. (2).

trated in **Fig. 1** was a real transition in surface tension caused either by slow changes in composition or restructuring of the surface. These data suggest that further study of interfacial behavior at elevated temperature would be valuable.

The temperature range of the pendant drop method is limited by the need for accurate density measurements, and the requirement for accurate temperature control of the cell. The severe change in viscosity over large temperature ranges makes forming and controlling drops very challenging. The method is unsuitable in the reacting regime of 350-400°C due to the evolution of vapor, which would generate bubbles in the injection tube and droplet. Any bubbles would invalidate the density used in the calculation. At higher temperatures, the time to establish a drop would be too large relative to the reaction time. The method could be extended to high pressures, and has been used for this purpose at low temperature up to 14 MPa<sup>6)</sup>, but the limitations on reactions prevent the method from being used at hydroconversion conditions.

Millette *et al.*<sup>7)</sup> suggested the use of the maximum bubble pressure method for measuring surface tension at high pressures in opaque liquids. This method is based on the pressure required to create a bubble at the tip of a capillary tube, which is related to the surface tension and the bubble radius:

$$P_{\text{bubble}} - P_{\text{fluid}} = \frac{2\sigma}{r} \quad (4)$$

where  $r$  is the radius of the bubble. The use of two submerged capillaries of different radii allows correction for hydrostatic head, and a correction is used for non-spherical bubble formation at the tip of a capillary. Millette *et al.*<sup>7)</sup> reported calibration data on *n*-octane to 225°C at 13.8 MPa, and claimed useful results on oils up to 350°C. Unfortunately, neither the data nor the validation for the higher temperature results were presented. The temperature limit in this case was the onset of reaction, which made the bubble pressure sensitive to volatile components. This result is consistent with the limitations on using this method for mixtures of any kind<sup>8),9)</sup>.

Aminu *et al.*<sup>10)</sup> described a new method for measuring surface tension that was designed specifically for

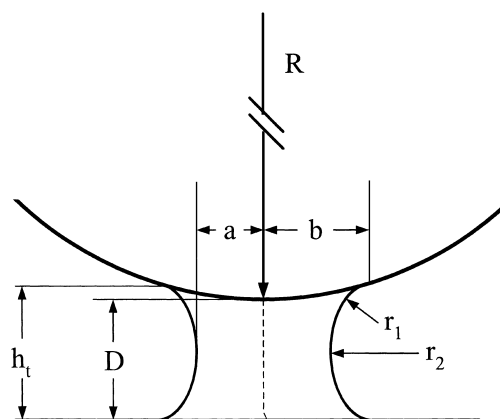
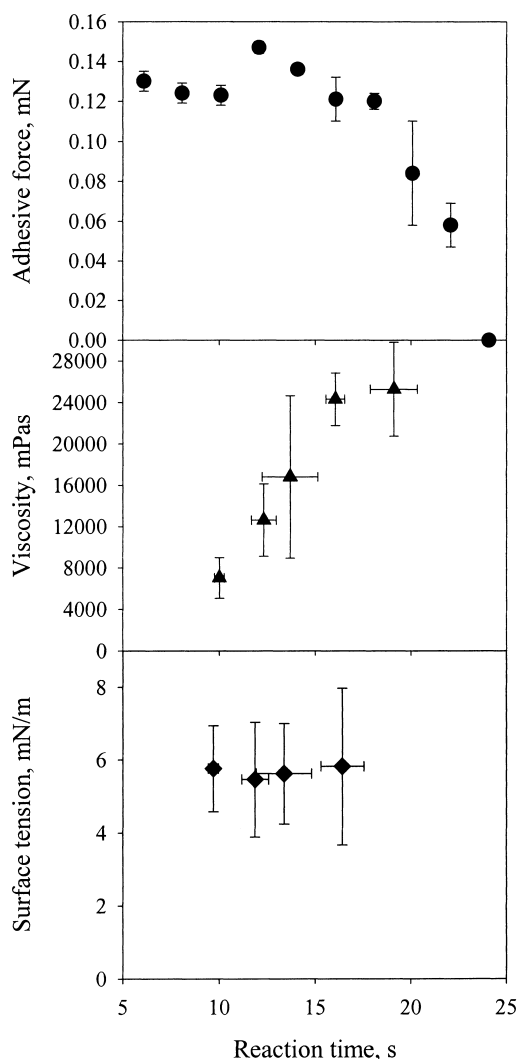


Fig. 3 Liquid Bridge between a Rod and a Plate, Which Shows the Same Geometry as a Bridge between Crossed Cylinders

high-temperature reacting systems. By forming a liquid bridge of vacuum residue between two rods of Ni-Fe alloy, they were able to achieve rapid heating to a controlled temperature by using the Curie-point effect in an induction coil. This technique was suitable for measurements at fluid coking conditions, where reactions occur in thin films on a hot coke surface at temperatures over 500°C. By heating the vacuum residue as a thin film of *ca.* 10 μm in an inert atmosphere, then touching two rods to form a liquid bridge, cracked vapor products escaped from the liquid phase. The force due to the liquid bridge was measured by mounting one rod on a pivot spring, which gave a linear relation between force required to displace the rod and its position. The geometry of a liquid bridge between two cylindrical rods is equivalent to a bridge between a sphere and a plane, as illustrated in **Fig. 3**. For a thin film of liquid on a rod of diameter 1-2 mm, the liquid bridge was much shorter than its width ( $D < b$ ) and the governing relation was:

$$F_s = 4\pi R\sigma \quad (5)$$

where  $F_s$  is the force and  $R$  is the radius of the rod. Using this method, they measured surface tension of Athabasca vacuum residue in the range from 310-530°C. The main difficulty that they encountered was noise in the signals due to the induction coil.



The reaction time was defined as the total heating time less the time to reach 400°C. Error bars are standard deviations for three repeat experiments.

Fig. 4 Properties of Reacting Athabasca Vacuum Residue at 503°C, from Aminu *et al.*<sup>10)</sup>

Asprino<sup>11)</sup> eliminated the noise and measured values over the same range. The data for the non-reacting regime (temperatures below 400°C) are illustrated in Fig. 2, for comparison with the data of Li *et al.*<sup>2)</sup>. At higher temperatures, the surface tension continued to decline to only 2 mN/m at 530°C. One of the most surprising observations of Aminu *et al.*<sup>10)</sup> was the insensitivity of the surface tension to reaction. The data of Fig. 4 illustrate the lack of change over a period of 7 s, during which time significant cracking and conversion of the residue was taking place at 503°C.

The same technique was used by Aminu *et al.*<sup>10)</sup> to measure adhesive force, which was a direct indication of whether sufficient liquid remained to form a liquid bridge. By pulling the rods apart, they measured the

force required to break the bridge. As illustrated in Fig. 4, the force was relatively constant through the initial stage, then it decreased to zero force after 24 s of reaction. At this point, the reaction of the liquid was so extensive that either the quantity was so low or the viscosity was so high that a liquid bridge could not form, and no adhesion driven by surface tension could occur between the rods used for measurement.

The work of Li *et al.*<sup>2)</sup> and Aminu *et al.*<sup>10)</sup> illustrate complementary approaches to measuring surface tension at temperatures relevant to process conditions. Further work is required to develop new methods that could be applied to the high-pressure conditions relevant to hydroconversion processes.

#### 4. Viscosity

Conventional viscosity measurements, using techniques such as Couette or capillary viscometers and parallel-plate rheometers, can be used to measure viscosity and non-Newtonian fluid properties at temperatures up to 1000°C, limited only by the heating capabilities of the instrument. Temperatures of up to 2000°C can be handled without contamination using the gas-film levitation method, which examines the deformation of a liquid drop suspended on a film of gas<sup>12)</sup>.

Extensive studies of the rheology of petroleum and coal pitches have been carried out *in-situ* during the formation of mesophase. Most published studies are on pitches derived from coal<sup>13)–15)</sup>, or naphthalene<sup>16)</sup>. Petroleum pitches have qualitatively similar chemical and physical properties<sup>17)</sup>, with some differences in aliphatic and naphthenic components that give better fiber-manufacturing properties<sup>18)</sup>. These pitches are thermoplastic mixtures of alkyl aromatics and naphthoaromatics derived from thermal or catalytic cracking processing of crude oil fractions, particularly vacuum residue and aromatic oils from fluid catalytic cracking. The transformation of these pitches to mesophase at 300–400°C is important in the manufacture of carbon fibres. The rheology of the fluid during this transformation is complex due to the formation of the liquid-crystalline mesophase as an emulsion in the pitch material. Due to their prior thermal history, these pitches are much less reactive than typical vacuum residues, which allows the use of conventional rheological measurements.

In contrast to pitches, vacuum residues evolve large volumes of cracked gases and vapors at the temperatures listed for the processes in Table 1. Evolution of bubbles, for example in the types of rheometers used to study mesophase formation<sup>17)</sup>, renders the measurement of liquid properties invalid. Small droplets of vacuum residue could possibly be observed and analyzed by the gas-film levitation method, but even this method would likely be susceptible to bubble formation at 500°C if

the liquid droplet were of radius 50  $\mu\text{m}$  or larger<sup>19)</sup>, which is too small for the observation of deformation required to calculate viscosity.

Aminu *et al.*<sup>10)</sup> used the forces exerted by liquid bridges to determine viscosity, in addition to the surface tension. As illustrated in **Fig. 3**, the geometry of a liquid bridge between crossed cylinders can be viewed as a sphere and a plane<sup>20)</sup>. The total force on the liquid bridge is the sum of the surface force and the viscous force<sup>21)–24)</sup>.

$$F_T = F_s + F_v \quad (6)$$

The total force,  $F_T$  is measured experimentally, while the contributions from surface forces and viscous forces are  $F_s$  and  $F_v$ , respectively. When the liquid bridge elongates, so that  $D > b$ , then the force becomes:

$$F_s = \pi\sigma b \left(1 + \frac{b}{r_1}\right) \quad (7)$$

similar to the relationships given by Fairbrother and Simons<sup>25)</sup> and Pitois *et al.*<sup>23),24)</sup>. When the bridge is very short, with  $D < b$ , then Eq. (5) describes the force, as discussed above. For a cylindrical bridge of fixed volume, the viscous force is given as<sup>23),24)</sup>:

$$F_v = \frac{3\pi\mu R^2}{D} \frac{dD}{dt} \quad (8)$$

Aminu *et al.*<sup>10)</sup> used crossed cylinders that were coated with a thin liquid film of thickness,  $\delta$ . When the two rods touched a liquid bridge was formed. The volume of this bridge varied as it was stretched, due to the flow of liquid from the film into and out of the bridge. Rather than solving the full equations for changes in the volume of the liquid bridge, Aminu *et al.*<sup>10)</sup> used dimensional analysis to give an empirical solution for the viscous force. The equations for the forces were non-dimensionalized by multiplication by  $D/(R^2 \cdot \sigma)$ . The dimensionless surface force then became:

$$F_{s,D} = 4\pi \frac{D}{R} \quad \text{for } D < b \quad (9)$$

$$F_{s,D} = \frac{\pi b D}{R^2} \left[1 + \frac{b}{r_1}\right] \quad \text{for } D > b \quad (10)$$

The dimensionless viscous force from Eq. (8) was proportional to the capillary number, defined in this case as:

$$Ca = \frac{\mu}{\sigma} \frac{dD}{dt} \quad (11)$$

The Reynolds number was less than 2; therefore, inertial effects were not significant. Allowing for empirical dependence on the thickness of the liquid film,  $\delta$ , and the length of the liquid bridge,  $D$ , Aminu *et al.*<sup>10)</sup> proposed the following semi-empirical expression:

$$F_{v,D} = k_1 Ca \left(\frac{\delta}{R}\right)^{k_2} \left(\frac{D}{R}\right)^{k_3} \quad (12)$$

where  $k_1$ ,  $k_2$  and  $k_3$  were empirical constants. The total force on a liquid bridge for  $D \geq b$  was

$$F_{T,D} = \frac{\pi b D}{R^2} \left(1 + \frac{b}{r_1}\right) + k_1 Ca \left(\frac{\delta}{R}\right)^{k_2} \left(\frac{D}{R}\right)^{k_3} \quad (13)$$

The coefficients were determined from a series of experiments with calibration oils of known viscosity (1–22 Pa·s), giving best-fit values of  $k_1 = 400.0$ ,  $k_2 = 0.752$  and  $k_3 = 0.677$ . Asprino<sup>11)</sup> extended the range of the calibration to ca. 100 Pa·s, with no change in the constants. Experimentally, they observed that when the bridge was fully elongated, just before it broke, the contribution of the surface force was insignificant:

$$F_{T,D} = 400 Ca \left(\frac{\delta}{R}\right)^{0.752} \left(\frac{D}{R}\right)^{0.677} \quad (14)$$

In order to apply this relation to reacting systems, they correlated the film thickness,  $\delta$ , with kinetic data for liquid remaining as a function of reaction time and temperature from Gray *et al.*<sup>26)</sup>. Rearranging Eq. (14) to solve for viscosity gives:

$$\mu = \frac{F_T D}{400 \cdot \frac{dD}{dt} \cdot R^2 \left(\frac{\delta}{D}\right)^{0.752} \left(\frac{D}{R}\right)^{0.677}} \quad (15)$$

The change in fluid properties with at 503°C is illustrated in **Fig. 4**. The top panel shows the adhesive force, which was the maximum force to pull the rods apart and break the liquid bridge. Equation (15) was used to calculate the viscosity from the adhesive force ( $F_T$ ), the thickness of the liquid film ( $\delta$ ), the length of the liquid bridge ( $D$ ), the rate of elongation of the liquid bridge ( $dD/dt$ ), and the radius of the rod ( $R$ ). The values of  $D$  and  $dD/dt$  were determined from the measured relative positions of the two rods as a function of time. The measured forces on the liquid bridges at the time of breakage were relatively constant with time for the first 20 s, as illustrated in **Fig. 4**, therefore, the diminishing thickness of the liquid film ( $\delta$ ), the changes in bridge length ( $D$ ), the rate of extension of the bridge ( $dD/dt$ ), and the increasing viscosity were compensatory.

All of the experiments in the temperature range of 400–530°C gave similar curves for adhesive force and viscosity to **Fig. 4** as a function of reaction time. The only difference was that the time scale for drying out the film decreased as the temperature was increased, where dry-out time was defined as the reaction time to produce a film with no measurable adhesive force. The time for a reacting film to dry out decreased with increasing temperature from 240 s at 400°C to 24 s at 503°C (see **Fig. 4**) to 14.4 s at 530°C. As illustrated in **Fig. 5**, viscosity increased significantly with reaction time at all temperatures to values in the range of  $3 \times 10^4$  to  $5 \times 10^4$  mPa·s. Aminu *et al.*<sup>10)</sup> pointed out that the viscosities were apparent values, because non-Newtonian behavior of the reacting material during coke formation could not be ruled out.

According to data from Aminu *et al.*<sup>10)</sup>, the viscosity

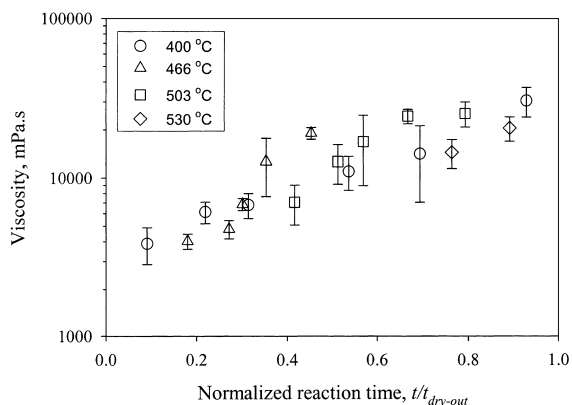


Fig. 5 Viscosity of Reacting Athabasca Vacuum Residue as a Function of Normalized Reaction Time, Using Time to Dry out the Liquid Film,  $t_{dry-out}$ , as a Scaling Variable

of the unreacted Athabasca vacuum residue was 1 to 2 mPa·s, based on extrapolation of measurements below 280°C. The rapid increase in viscosity from 1 to 2 mPa·s to  $10^4$  mPa·s with increasing time of reaction was consistent with evaporation of more volatile components from the liquid film and polymerization of liquid components, driven by thermal cracking reactions, leading to coke formation.

Aminu *et al.*<sup>10)</sup> showed that the data for viscosity as a function of time at different temperatures could be reduced to a single, approximately linear, relationship as illustrated in **Fig. 5**. The viscosity data from experiments at 400-530°C were plotted against the normalized reaction time, defined as the reaction time divided by the time to obtain a dry film.

## 5. Contact Angle

As indicated by Eq. (1), the contact angle depends on both the properties of the phases in the vacuum residue during processing, but also on the surface properties of the solid phases. Perhaps for this reason, contact angle measurements for vacuum residues and its sub-fractions at processing temperatures have not been reported. Some work has been done on the contact angle of pitch materials with coke solids, in order to assess binder properties<sup>27),28)</sup>. By examining the time for droplets of pitch to flow into powdered coke, these studies give results that depend on viscosity, surface tension of the fluid, dynamic contact angle at the liquid-solid contact, and the pore characteristics of the powdered solid. Consequently, this approach does not give a clear indication of contact angle alone. Measurements of liquid contact angle on coke surfaces would be relevant to liquid fouling behavior when vapor is the continuous phase, as in fluid coking or residue FCC. Extension of the methods of Aminu *et al.*<sup>10)</sup> to contact angle measurements would be relatively straightforward.

A more challenging problem is measurement of three-phase contact angle between liquid, coke precursors or mesophase, and reactor internals or catalyst surfaces. Such measurements would be relevant to fouling of furnaces and heat exchangers, and in hydroconversion processes. The difficulties in this case include the ongoing reactions in the fluid phases, the composition of the solid surfaces which are usually either coke deposits or metal sulfides in refinery service, and the opacity of the vacuum residue material. The recent work of Zou and Shaw<sup>29)</sup> suggests that X-ray techniques could be adapted to such measurements. The challenge would be to obtain sufficient resolution of the interface to be able to fit the governing equations to the three-phase contact.

## 6. Future Research Challenges

The recent work of Aminu *et al.*<sup>10)</sup> has shown that vacuum residue properties can be measured *in-situ* during reactions at 400-530°C under selected physical conditions, and thereby provide valuable insight into the potential for fouling and adhesion behavior as a function of time. The biggest challenge for the future is to develop complementary methods for measuring surface tensions and viscosities in the liquid phase under conditions relevant to fouling, both at low pressure and under hydrogen pressure. Similarly, the measurement of contact angle on representative surfaces at processing conditions would provide important insights. The need in these measurements is to characterize the developing coke precursors, rather than the bulk liquid phase. For example, the fouling of furnace tubes in a delayed coker could be understood in terms of adhesion of coke precursors to the surface, if such methods were available. Expansion of the range and quality of these fluid property measurements will provide new tools for design and operation of residue conversion units.

### Nomenclatures

$a, b$	: dimensions of base of liquid bridge from Fig. 3	[m]
$d$	: characteristic length in dimensionless groups, usually drop or bubble diameter	[m]
$D$	: length of liquid bridge	[m]
$F$	: forces on due to liquid bridge	[N]
$g$	: gravitational acceleration	[m/s <sup>2</sup> ]
$h$	: height of liquid bridge from Fig. 3	[m]
$p$	: pressure	[Pa]
$r_1$	: radius of curvature from Fig. 3	[m]
$r$	: radius of bubble	[m]
$R$	: radius of cylinder or rod in Fig. 3	[m]
$t$	: time	[s]
$U$	: characteristic velocity in dimensionless groups	[m/s]
<Greeks>		
$\delta$	: liquid film thickness	[m]
$\theta$	: contact angle	[—]
$\mu$	: viscosity	[Pa·s]
$\rho$	: density	[kg/m <sup>3</sup> ]

$\sigma$  : surface tension or interfacial tension [N/m]  
 <Subscripts>  
 D : dimensionless  
 G : gas or vapor  
 L : liquid or fluid  
 s : surface  
 S : solid  
 T : total  
 v : viscous

### References

- 1) Bozzano, G., Dente, M., Faravelli, T., Ranzi, E., *Appl. Therm. Eng.*, **22**, 919 (2002).
- 2) Li, X., Elliott, J. A. W., McCaffrey, W. C., Yan, D., Li, D., Famulak, D., *J. Colloid Interface Sci.*, in press (2005).
- 3) Cheng, P., Li, D., Boruvka, L., Rotenburg, Y., Neumann, A. W., *Colloids Surf.*, **43**, 151 (1990).
- 4) Li, D., Cheng, P., Neumann, A. W., *Adv. Colloid Interface Sci.*, **39**, 347 (1992).
- 5) Poling, B. E., Prausnitz, J. M., O'Connell, J. P., "The Properties of Gases and Liquids," 5th ed., McGraw-Hill, New York (2000).
- 6) Schramm, L. L., Fisher, D. B., Schurch, S., Cameron, A., *Colloids Surf. A*, **94**, 145 (1995).
- 7) Millette, J. P., Scott, D. S., Reilly, I. G., Majerski, P., Piskorz, J., Radlein, D., deBruijn, T. J. W., *Can. J. Chem. Eng.*, **80**, 126 (2002).
- 8) Harkins, W. D., in Weissberger, A. (Ed.), "Physical Methods of Organic Chemistry," Vol. 1, Interscience, New York (1959), p. 757.
- 9) Padday, J. F., in Matijevec, E. (Ed.), "Surface and Colloid Science," Vol. 1, Wiley-Interscience, New York (1969), p. 101.
- 10) Aminu, M. O., Elliott, J. A. W., McCaffrey, W. C., Gray, M. R., *Ind. Eng. Chem. Res.*, **43**, 2929 (2004).
- 11) Asprino, O., M. Sc. Thesis, University of Alberta, Canada, Fall 2004.
- 12) Perez, M., Salvo, L., Seury, M., Brechet, Y., Papoular, M., *Phys. Rev. E*, **61**, 2669 (2000).
- 13) Collett, G. W., Rand, B., *Fuel*, **57**, 162 (1978).
- 14) Fitzer, E., Kompalik, D., Yudate, K., *Fuel*, **66**, 1504 (1987).
- 15) Huttinger, K. J., Wang, J. P., *Carbon*, **29**, 439 (1991).
- 16) Yoon, S.-H., Korai, Y., Mochida, I., Kato, I., *Carbon*, **32**, 273 (1994).
- 17) Rand, B., *Fuel*, **66**, 1491 (1987).
- 18) Mochida, I., Toshima, H., Korai, Y., Varga, T., *J. Mater. Sci.*, **25**, 3484 (1990).
- 19) Gray, M. R., Le, T., McCaffrey, W. C., Berruti, F., Soundararajan, S., Chan, E., Huq, I., *Ind. Eng. Chem. Res.*, **40**, 3317 (2001).
- 20) Fisher, L. R., Israelachvili, J. N., *J. Colloid Interface Sci.*, **80**, 528 (1981).
- 21) Mazzone, D. N., Tardos, G. I., Pfeffer, R., *Powder Tech.*, **51**, 71 (1987).
- 22) Ennis, B. J., Li, J., Tardos, G. I., Pfeffer, R., *Chem. Eng. Sci.*, **45**, 3071 (1990).
- 23) Pitois, O., Moucheron, P., Chateau, X., *J. Colloid Interface Sci.*, **231**, 26 (2000).
- 24) Pitois, O., Moucheron, P., Chateau, X., *Eur. Phys. J. B*, **23**, 79 (2001).
- 25) Fairbrother, R. J., Simons, S. J. R., *Part. Part. Sys. Char.*, **15**, 16 (1998).
- 26) Gray, M. R., McCaffrey, W. C., Huq, I., Le, T., *Ind. Eng. Chem. Res.*, **43**, 5438 (2004).
- 27) Lahaye, J., Ehrburger, P., *Fuel*, **64**, 1187 (1985).
- 28) Couderc, P., Hyvernay, P., Lemarchand, J. L., *Fuel*, **65**, 281 (1986).
- 29) Zou, X.-Y., Shaw, J. M., *Petrol. Sci. Tech.*, **22**, 759 (2004).

## 要 旨

### 減圧残さおよびアスファルテンのプロセス条件下における流体特性の測定

Murray R. GRAY, Janet A. W. ELLIOTT, William C. McCAFFREY

Dept. of Chemical and Materials Engineering, University of Alberta, Edmonton, AB T6G 2G6, CANADA

表面張力および粘度といった流体特性，ならびに接触角で表される流体-固体の相互作用は，石油やオイルサンドピチュメンから得られる減圧残さ留分を処理する際に観察される種々の現象に影響を与える因子として重要である。たとえば，これらの流体特性を代表的な処理条件下で直接測定することによって，水素化処理プロセス装置内でのガスホールドアップや加熱炉チューブ内のファウリング生成といった装置設計や運転に関

しての重要な情報を得ることができる。本総説は，減圧残さの高温・高圧下での流体特性の測定に関しての取組みを解説したものである。現在まで，低圧条件下，530℃までの温度領域における減圧残さの表面張力と粘度の測定については大きな進展が見られたが，今後，接触角の測定や高圧条件下での流体特性の測定方法の開発に対してさらなる努力が必要である。